ELSEVIER

Polymer 41 (2000) 4957–4964

polymer

Molecular order and phase transitions in smectic poly(ester imide)s based on trimellitimide

C. Wutz*

Institut für Technische und Makromolekulare Chemie, Universität Hamburg, Bundesstrasse 45, D-20146 Hamburg, Germany

Received 4 November 1998; received in revised form 13 May 1999; accepted 18 May 1999

Abstract

Poly(ester imide)s have been derived from aminobenzoic acid (PEI **1**), respectively, aminocinnamic acid (PEI **2**), trimellitic acid, and α,ω-dihydroxyalkanes to form various smectic liquid-crystalline (LC) and smectic-crystalline phases, dependent on the type of mesogen, spacer length, and thermal treatment. In this study, the phase behaviour and molecular structure of these PEI has been investigated by polarising microscopy, DSC, X-ray scattering, light scattering and solid-state NMR.

The temperature gap of the monotropic LC-phase becomes narrower with increasing spacer length. If the LC-phase is lost completely, the smectic-crystalline phase develops directly from the isotropic melt with a three-dimensional spherulitic superstructure of several μm diameter. In contrast, the Avrami-evaluation of the crystallisation from the LC-phase indicates two-dimensional crystal growth starting from disclination centres. The development of a long period reflection in the small angle X-ray scattering reveals a lamellar superstructure of 100–400 Å. Each lamella contains a number of smectic-crystalline layers, while the interlamellar regions are amorphous.

X-ray fibre patterns demonstrates that the PEI **1** form orthogonal smectic phases (S_A, S_B, S_E), unlike PEI **2**, which form tilted phases (S_C,S_H). The ^{13}C NMR results indicate a uniform spacer conformation in the LC-phase corresponding to an alternate-*trans* model, while the smectic-crystalline phase contains ordered *trans–trans*-conformations, as well as completely disordered sequences.

Keywords: Smectic; Spherulites; X-ray scattering

1. Introduction

In order to produce materials with outstanding mechanical properties, polymers with stiff, wholly aromatic main-chains—so-called rigid rod molecules—have been developed. They were synthesised by the polycondensation of bifunctional aromatic carbon acids, alcohols, amines, etc. From theoretical predictions of Flory [1] and practical experience, it is well known that such stiff macromolecules are neither meltable nor soluble. To overcome these drawbacks, different concepts have been developed to lower the melting point and increase solubility. For example, flexible side-chains attached to the rigid backbone can act as a *bounded solvent* [2,3]. This molecular architecture usually forms so-called sanidic or biaxial-nematic phases [4]. Further, kinks or side steps can be inserted into the linear molecular structure [5,6], for example, by the substitution of terephthalate with isophthalate or naphthalene dicarboxylate units. Finally, flexible segments can be introduced into the main chain [7] via condensation with aliphatic diols, dicarbon acids, or diamines. The resulting segmented polymers often form liquid-crystalline (LC) phases [8,9].

With regard to poly(ester imide)s derived from aminobenzoic acid trimellitimide (PEI **1**), respectively, aminocinnamic acid trimellitimide (PEI **2**), and α,ω-dihydroxyalkanes (Fig. 1), the difference in the polarities between the rigid, mesogenic imide blocks and the flexible alkane spacers is particularly large. As a result of their amphiphilic nature, these molecules tend to form smectic layers [10,11]. It should be emphasised that the term *smectic* does not imply liquid-crystallinity. In addition to the two smectic LC-phases S_A and S_C, a number of so-called higher-ordered smectic phases exist, which are denoted as S_B, S_E, S_F, and S_H, depending on the lateral order of the mesogens and their orientation with respect to the layer plane (Fig. 2). This classification has been adopted from the low molecular weight liquid-crystals [12]. However, in contrast to the low molar mass compounds, these higher-ordered smectic phases are solid in polymers, since the molecular chains, which pass several smectic layers prevent the layers from sliding off.

* Tel.: +49-40-42838-6004; fax: +49-40-42838-6008.
E-mail address: wutz@vxdesy.desy.de (C. Wutz).

0032-3861/00/$ - see front matter
PII: S0032-3861(99)00561-3

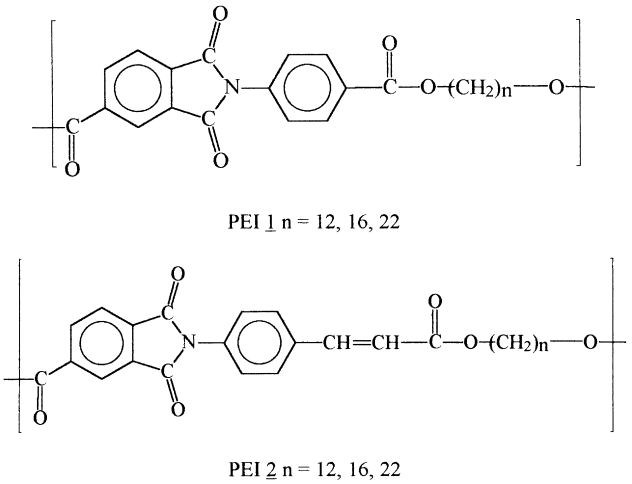

Fig. 1. Chemical structures of the PEI **1** and **2**.

In all smectic phases, the regular layer structure of 20–40 Å gives rise to a reflection in the middle-angle X-ray scattering (MAXS) at $2\theta = 1–5°$, dependent on the length of the mesogen and the spacer. In the LC-phase, an *amorphous halo* is detected in the wide-angle X-ray scattering (WAXS, $2\theta = 5–40°$) in lack of lateral positional order of the mesogens. In contrast, their regular packing in the higher-ordered smectic phases results in crystal reflections in the WAXS. Consequently, these phases have also been classified as *smectic-crystalline*, despite the substantial conformational disorder of the spacers [13].

Previous investigations [10,11,14–16] have demonstrated that the PEI **1** and **2** form different smectic phases, depending on the type of mesogen, the spacer length and the thermal treatment. If the PEI **1** and **2** display smectic LC-phases, they are only monotropic; that is, they form only during cooling of the isotropic melt. Upon further cooling, the transition into the smectic-crystalline phase occurs with orthorhombic or monoclinic mesogen packing. During heating, the crystals melt directly into the isotropic phase. Rapid quenching of the isotropic or LC melt freezes the LC-structure. Subsequent annealing above the glass transition temperature causes crystallisation once again. During this process, the PEI **1** $n \leq 12$ exhibit an interesting thermal behaviour. At first, they form a hexagonal smectic-crystalline phase, which transforms into the stable orthogonal phase at higher temperatures.

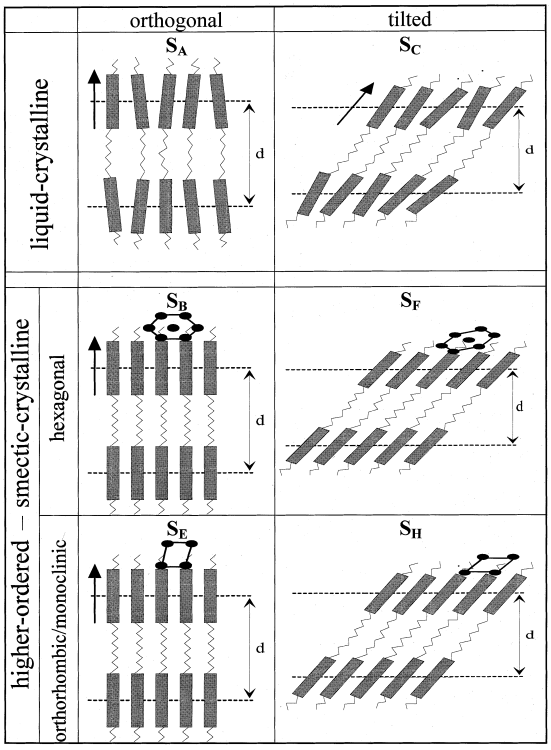

Fig. 2. Schematic representation of different smectic phases.

2. Experimental

2.1. Materials

All PEI samples studied were synthesised by Kricheldorf and co-workers (Hamburg, Germany). The synthetic route and the basic properties of the polymers have been published previously [10,11,17]. The polymers were dissolved in a mixture of trifluoroacetic acid and $CHCl_3$, precipitated into methanol and dried at 80°C. For the light scattering measurements, the polymers were fused between glass slides.

2.2. Measurements

Differential scanning calorimetry (DSC) traces were recorded with a Perkin–Elmer DSC-4 in aluminium pans at a cooling rate of 10°C/min.

The X-ray experiments were performed using the synchrotron radiation of the Deutsche Elektronen Synchrotron (DESY) in Hamburg, Germany, at a wavelength of $\lambda = 1.54$ Å. The time-resolved measurements of WAXS, MAXS and SAXS were carried out simultaneously with two position-sensitive detectors and 30 s acquisition time per frame. The X-ray fibre patterns were acquired by image-plates with 1–2 min exposure time. The fibre direction is vertical.

The H_V-light scattering patterns were determined using a Melles–Griot He/Ne-laser ($\lambda = 632.8$ nm) and a CCD camera. In order to eliminate speckles, the patterns were averaged over the four quadrants and smoothed. The polymer was fused between 0.17 mm glass plates.

The NMR spectra were recorded on a Bruker MSL 300 spectrometer (7.05 T) at a ^{1}H frequency of 300.13 MHz. ^{13}C solid state NMR using cross polarisation, magic angle spinning (CP/MAS) and dipolar decoupling was performed at 75.47 MHz using a double-bearing variable temperature Bruker MAS probe, 7 mm zirconium oxide rotors, 5000 Hz spinning rate, 1 ms contact time, and 4 s recycle delay. About 1000 acquisitions were averaged for each spectrum.

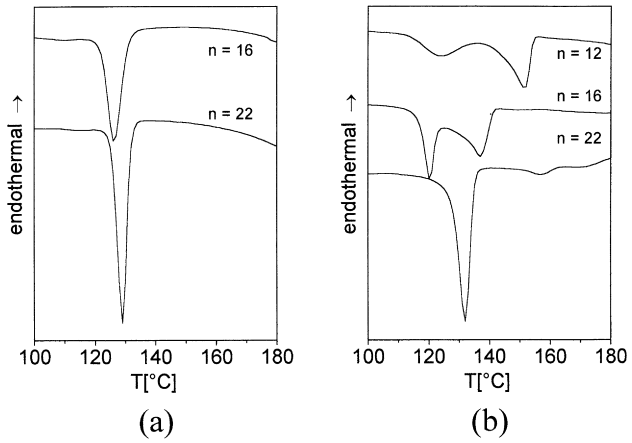

Fig. 3. DSC cooling traces of: (a) PEI **1**; (b) PEI **2** with different spacer length at a rate of −10°C/min.

3. Results and discussion

3.1. Smectic spherulites

In general, the PEI **1** and **2** form monotropic LC-phases. The DSC cooling traces of PEI **2** $n = 12$ and 16 (Fig. 3(b)) display two exothermal signals. The one at higher temperatures can be attributed to the formation of the smectic LC-phase. The low-temperature transition depends largely on the cooling rate, which indicates crystallisation. The *LC-gap* between the transitions becomes narrower with increasing spacer length *n*. For very long spacers, it vanishes completely and the smectic-crystalline structure forms directly from the isotropic melt. For PEI **1**, the LC-phase disappears at $n = 16$ (Fig. 3(a)), while for PEI **2** it is lost not before $n = 22$ (Fig. 3(b)). By substituting aminocinnamic acid for aminobenzoic acid, the double bond prolongates the rigid building block and, therefore, improves the mesogenic character of the molecule.

During the LC-phase formation, the whole sample becomes spontaneously anisotropic, and in the polarising microscope a typical LC-texture (schlieren, fan-shaped or grainy) is observed, which changes only slightly during subsequent crystallisation. However, if the crystallisation occurs directly from the isotropic melt, spherulites grow slowly out of the isotropic matrix (Fig. 4). This observation excludes an intermediate formation of a short-lived LC-phase, because it would make the whole sample anisotropic within seconds. However, time-resolved measurements of the X-ray scattering reveal that the development of the smectic-crystalline structure from the isotropic melt takes anywhere from a few minutes to several hours, depending on the temperature [18]. During this process, the layer reflection in the MAXS, indicating the smectic layers, and the crystal reflections in the WAXS develop simultaneously (Fig. 5). These measurements prove that liquid-crystallinity is not a prerequisite in the formation of a smectic layer structure. The kinetics of this process can be evaluated according to the Avrami law [19–21] (Eq. (1)), in which $I(t)$ is the integral intensity of the reflection representing the volume of the scattering structure, while I_{max} is the maximum intensity at the end of the process, k is the rate constant, and n the Avrami-exponent, which is related to the dimension of the growing entities.

$$I(t) = I_{max}(1 - e^{-kt^n}) \quad (1)$$

The resulting exponents of n close to 3 (see Ref. [18]) correspond with the formation of the three-dimensional spherulitic superstructure.

The particularity of these spherulites is their internal smectic order, which causes the layer reflection in the MAXS. Additionally, they possess an internal lamellar structure, similar to the spherulites of conventional, semi-crystalline polymers, which gives rise to a long-period reflection in the small-angle X-ray scattering (SAXS, $2\theta < 0.5°$). Obviously, these smectic spherulites are constructed of lamellar stacks with a *d*-spacing of 100–400 Å, each crystal lamella consisting of a number of smectic layers, as sketched schematically in Fig. 6. Some measurements indicate that the regions between the lamellae are probably amorphous. At the very least, they do not possess a smectic layer order (see Section 3).

As mentioned above, smectic spherulites occur, provided that the smectic-crystalline phase develops directly out of the isotropic melt. Under certain circumstances, this morphology can also be determined for polymers, which pass through a LC-phase during steady cooling (PEI **1** $n = 12$ and PEI **2** $n = 12, 16$) [22]. The basic requirement is a monotropic character of the LC-phase. In this case, the LC-phase is only meta-stable and is formed only during cooling due to the kinetic hindrance of the crystallisation. Fig. 7 depicts the thermodynamic relationships schematically. An enantiotropic, thermodynamically stable LC-phase (c) is always passed during heating and cooling. As a result of the lower activation energy, it develops much faster than the crystalline phase and, thus, determines the

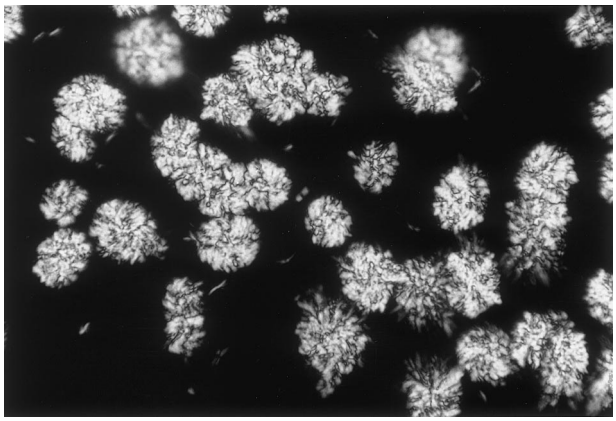

Fig. 4. Microscopic extinction pattern between crossed polars of PEI **1** $n = 22$ after 90 min at 150°C (20× magnification).

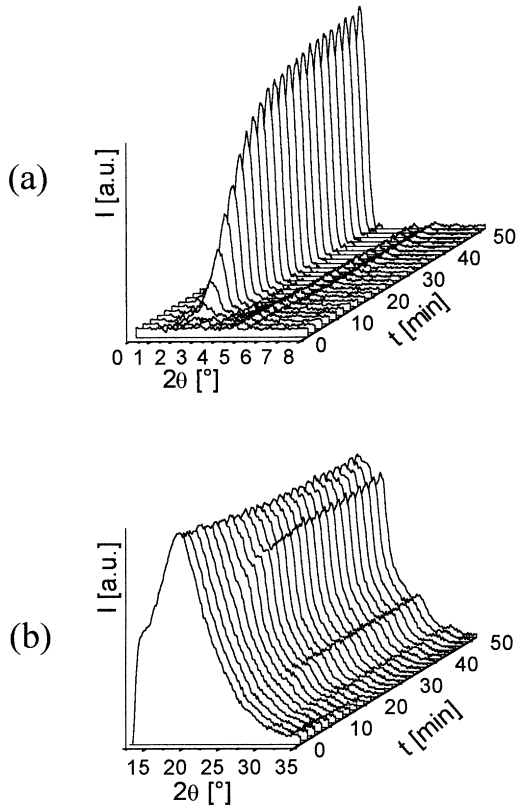

Fig. 5. Change of the: (a) MAXS; (b) WAXS of PEI **1** $n = 22$ during isothermal crystallisation at 140°C.

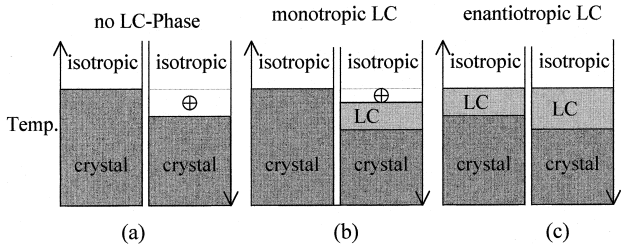

Fig. 7. Schematic representation of the phase behaviour of polymers: (a) without LC-phase; (b) passing through a monotropic LC-phase; (c) and forming an enantiotropic LC-phase.

microscopic texture. For monotropic LC-phases (b), the formation temperature during cooling is often lower than the melting point of the smectic-crystalline phase during heating. Within this temperature gap, the crystal is thermodynamically stable while the LC-phase is not. By cooling the isotropic melt and keeping it within this temperature gap isothermally, the smectic-crystalline phase develops slowly and that with a spherulitic superstructure. However, since these experiments have to be performed close to the melting point, the process can last from a few hours up to several days.

If the crystallisation proceeds very rapidly, i.e. during quenching, the spherulites remain small (~1 μm) and impinge on each other, so that it is impossible to differentiate them from a disturbed LC-texture by polarising microscopy. In this case, small angle light scattering (SALS) provides valuable information about the morphology. If the sample is transmitted by a linear polarised laser beam and the transmission direction of the following analyser is perpendicular, the spherulites give rise to a typical cloverleaf pattern with intensity maxima under ±45° relative to the polarisation direction as a rule (Fig. 8(a)) [23]. In contrast, the scattering of the disclinations in a LC-texture exhibits intensity maxima parallel to the direction of polarise and analyser (Fig. 8(b)) [24]. By these means, one can easily distinguish whether or not an intermediate LC-phase has been passed.

3.2. Orientation of the mesogens within the smectic layers and phase identification

As represented in Fig. 2, the smectic phases can be subdivided into orthogonal phases, in which the director is oriented parallel to the normal of the layer plane (S_A, S_B and S_E) and tilted phases (S_C, S_F, S_H). In principle, S_A- and S_C-phases can display different microscopic extinction patterns. However, the textures of LC-polymers are very often severely disturbed, so that a positive distinction is not possible. In contrast, the investigation of oriented samples by means of X-ray scattering provides information on the molecular structure and, therefore, allows a definite phase identification [25–27]. For the PEIs **1** and **2**, oriented samples can be easily obtained by drawing fibres from the melt. As a result of rapid cooling during this process, the

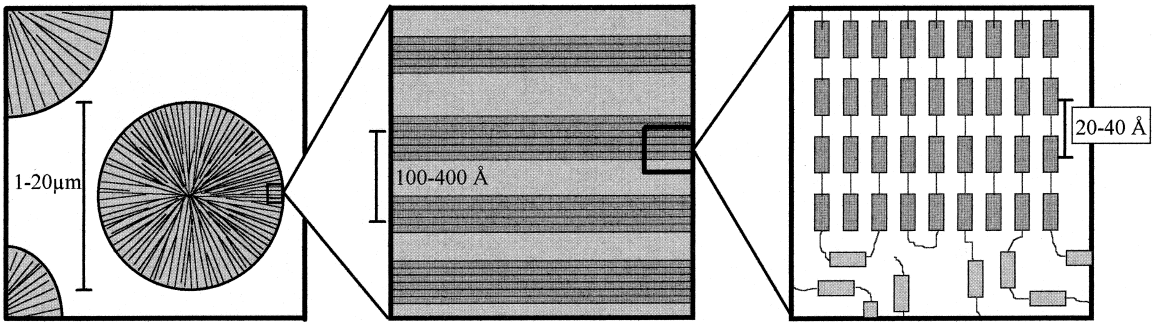

Fig. 6. Schematic representation of the smectic-spherulitic morphology.

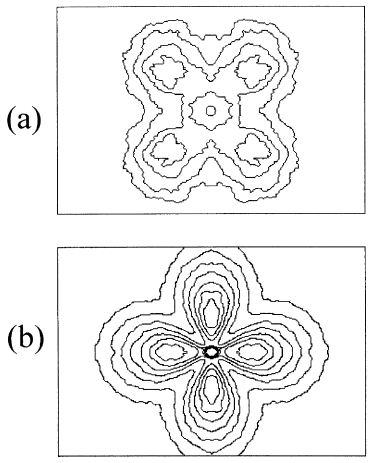

Fig. 8. H_V-light scattering patterns of: (a) PEI **2** $n = 16$ crystallised isothermally at 148°C for 1 h; (b) of PEI **2** $n = 12$ quenched rapidly from the melt.

oriented smectic LC-phase can be frozen. Annealing above the glass transition temperature produces the smectic-crystalline phase.

Since the molecular chains are aligned preferably parallel to the vertical fibre axis, the smectic layers of orthogonal phases are oriented horizontally, giving rise to meridional MAXS-reflections in the X-ray fibre pattern. In tilted smectic phases, the staggered arrangement of the mesogens forces the smectic layers to adopt an inclined orientation, resulting in an azimuthal splitting of the MAXS-reflections.

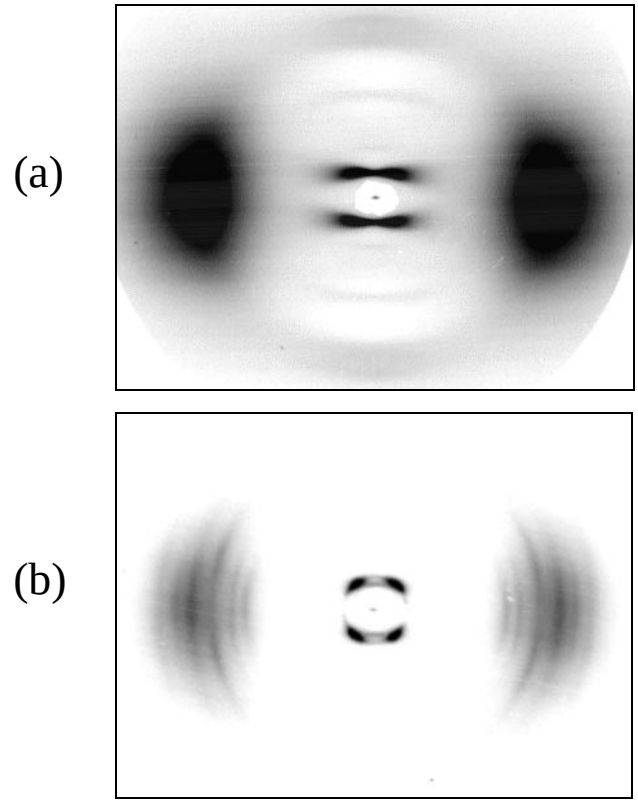

Fig. 9. X-ray patterns of a PEI **2** $n = 12$ fibre: (a) as drawn; (b) after annealing at 135°C for 15 min.

The simultaneous measurements of WAXS and MAXS powder patterns have already demonstrated that the layer reflection of the PEI **1** remains at the same position during the transitions between the smectic-LC phase, hexagonal, and orthorhombic phase. From this result, it can be assumed that no tilt occurs. The meridional layer reflections in the fibre patterns of the respective phases confirm that the PEI **1** form exclusively orthogonal phases (S_A, S_B, and S_E) [28].

In contrast, tilting between the mesogens and the smectic layers is observed in the smectic-crystalline phase of PEI **2**. As a result of the staggered arrangement of mesogens and spacers, the *d*-spacing becomes smaller and the MAXS-reflection shifts towards lower scattering angles (see Fig. 4 in Ref. [29]). In the X-ray fibre patters of PEI **2** $n = 12$ in Fig. 9, one can recognise that the frozen smectic LC-phase (a) displays split MAXS-reflections. Hence, it should be classified as a S_C-phase. However, the layerline shape of the MAXS-reflections indicates a poor lateral extension of the smectic layers [28]. Those phases are referred to as "poorly ordered smectics" [25].

During annealing, the development of the equatorial WAXS-reflections is due to the transition into the smectic-crystalline phase (Fig. 9(b)). The resulting split MAXS-reflections are now much sharper, because the lateral extension of the smectic layers is increased by the fitting of mesogens into the crystal lattice. The splitting angle of 40° corresponds to the molecular tilt angle between the mesogen axis and the normal of the smectic layer plane. Consequently, this structure is a S_H-phase, which can also be denoted as a two-dimensional crystal with a monoclinic lattice. During the transition, the MAXS-reflections shift outwards along a line parallel to the equator. Thus, the radial scattering angle increases as observed in the powder patterns, whereas the meridional component remains constant, since it corresponds to the length of the repeating unit. Together with the equatorial WAXS-reflections, this observation indicates that the mesogens are not tilted with respect to the fibre axis, as has been observed in other smectic polymers [30]. Moreover, a longitudinal reptation and a staggered arrangement of the mesogens orients the smectic-crystalline layers under 40° relative to the fibre axis. A detailed analysis of PEI X-ray fibre patterns will be published soon [28].

3.3. Crystallisation from the LC-Phase

The transition from the smectic-LC-phase to the smectic-crystalline phase results not only in the growth of WAXS crystal reflections, but additionally in the development of a SAXS. The long period reflection indicates the existence of a lamellar two-phase-system with *d*-spacings of 100–400 Å, as concluded previously for the smectic spherulites. Obviously, the molecular order of the smectic-crystalline phase is virtually independent of whether it develops from

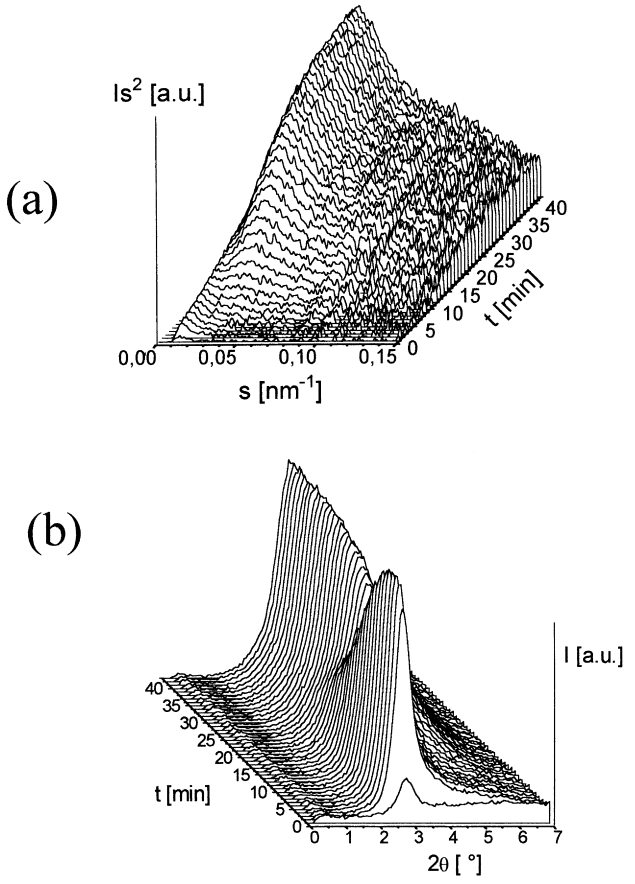

Fig. 10. Development of: (a) SAXS; (b) MAXS during isothermal crystallisation of PEI **2** $n = 12$ at 145°C.

the isotropic melt with a spherulitic superstructure or within a LC-texture. However, it is questionable whether the mechanism and the kinetics are the same.

Each crystal lamella is constructed of a few smectic layers with regularly packed mesogens and has a higher density than the disordered interlamellar regions. For the development of this structure from the smectic LC-phase, two different molecular mechanisms can be proposed [31]:

On the one hand, the pre-order of the mesogens by the smectic layering can persist and the mesogens align with the nearest neighbour to build a crystal lattice. In this case, only local motion and no long-range reorientation of chain segments would be necessary. The activation energy would be low, and the process would proceed rapidly, more or less independent of temperature. Indeed, all smectic layers could crystallise in this case, thus preventing the formation of a two-phase system. However, if crystallisation is prevented in parts of the sample as a result of molecular constraints, these parts would be distributed rather statistically, resulting only in a diffuse SAXS. Further, they would probably keep their smectic layer order.

The second mechanism assumes a nucleation-induced crystallisation, in which the crystal lamellae grow mainly by folding of the molecular chains, as occurs during the crystallisation of conventional, semi-crystalline polymers from the isotropic melt. The surface free energy of this *folded crystal* would be much lower than that of the *fringed crystal* described above. Chain foldings in the smectic-crystalline phase have already been considered by Watanabe et al. to explain the SAXS reflection of a polyester fibre [32]. Since chain foldings are rather rare in a LC-phase, they have to be generated during the crystal growth by long-range reptations or diffusions of chain segments.

Both mechanisms can be distinguished by investigating the isothermal crystallisation of the PEI **2**. As mentioned in Section 2, the position of the layer reflection in the MAXS changes during crystallisation of these polymers. PEI **2** $n = 12$ was cooled rapidly from the isotropic melt (200°C) to 145°C, yielding the smectic LC-phase, and was kept there isothermally. Fig. 10 illustrates the development of the SAXS (a) and the MAXS (b) detected simultaneously with 30 s acquisition time per frame. The first frame shows that the isotropic melt produces neither SAXS nor MAXS reflections as expected. In the second frame, when the temperature of 145°C is reached, the MAXS reflection at $2\theta = 2.9°$ indicates that the smectic LC-phase is formed spontaneously. In contrast, the long-period reflection in the SAXS indicating the smectic-crystalline phase develops very slowly. Depending on temperature, the half time amounts from several minutes up to a few hours. Along with the SAXS intensity, the MAXS-reflection of the smectic-crystalline layers develops at $2\theta = 3.6°$. Further, one can clearly see that the layer reflection of the smectic LC-phase vanishes completely during crystallisation. It can be conclude that the interlamellar regions have lost their smectic-LC layer-order during crystallisation. More detailed investigations of the smectic-crystalline phase will be published elsewhere [33,34].

Together with the slow and temperature-dependent kinetics of this process, these observations support the second mechanisms of crystallisation from the LC-phase. The smectic order of the mesogens in the LC-phase may induce nucleation. However, during the growth of the crystal lamellae, an entirely novel smectic layer system is formed. The generation of backfoldings at the lamella surface requires long-range chain reptations and diffusions, resulting in high activation energy. In the course of this reorientation process, entanglements occur that restrict crystallisation and destroy the smectic layering in the interlamellar regions. The decrease of local molecular order is, of course, unusual but does not contradict the thermodynamic rules. The regular packing of the mesogens within the crystal lamellae gains much more enthalpy than the loss of the smectic LC-order between the lamellae costs [35]. The destruction of the layering is equivalent to a molecular mixing of mesogens and spacers.

The kinetics of this process can also be evaluated based on the model of Avrami [19–21], in order to study the dimensionality of the crystal growth. For this purpose, the PEI **1** are more suitable than the PEI **2**, because their

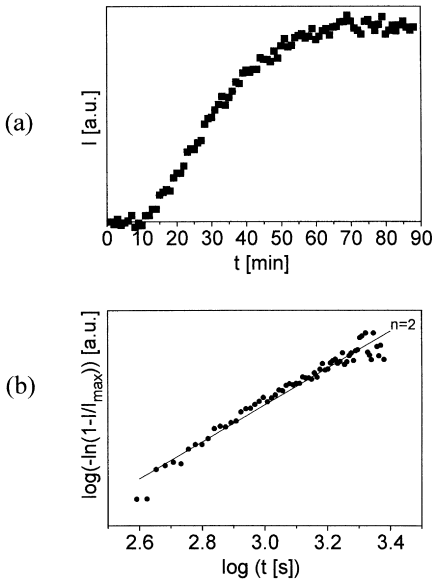

Fig. 11. Integral intensity of the WAXS-reflection I as a function of time during isothermal crystallisation of PEI **1** $n = 12$: (a) at 140°C; (b) corresponding Avrami-plot.

WAXS-reflections are stronger. Fig. 11 depicts the intensity of the crystal reflections as a function of time (a) and the corresponding Avrami-plot (b) for the isothermal crystallisation of PEI **1** $n = 12$ out of the LC-phase at 140°C. The resulting exponent of $n = 2$ is typical for a crystallisation originating from one-dimensional nuclei, which are the centres of disclinations in the LC-texture [36]. As mentioned above, the microscopically observed LC-texture

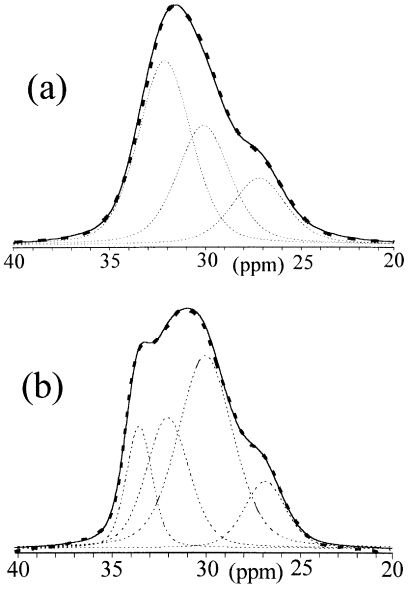

Fig. 12. Expanded ^{13}C NMR CP/MAS spectra of PEI **2** $n = 16$ at 20°C in: (a) the frozen smectic LC-phase; (b) in the smectic-crystalline phase. The thick dotted lines represent the experimental data; the thin dotted lines are the individual components of the deconvolution and the thin straight line is the sum.

of the PEIs is quite disturbed. Therefore, the high density of 1D nuclei at the disclination centres dominates the dimensionality of the crystal growth, whereas the influence of 2D nuclei at the domain walls inducing 1D crystal growth can be neglected.

3.4. Spacer conformation

In contrast to a true, three-dimensional crystal, the spacers of the smectic-crystalline phase are conformationally disordered. As a consequence, the positional order of the mesogens between adjacent layers is lost. The conformation of the spacer segments can be determined by means of ^{13}C solid-state nuclear magnetic resonance (NMR). Under the conditions of cross-polarisation (CP), magic angle spinning (MAS) and dipolar decoupling (DD), the ^{13}C chemical shift of a methylene carbon in an alkane chain is sensitive to the conformation of the two adjacent bonds via the γ-*gauche*-effect [37]. A *gauche* conformation causes more shielding of the carbon under observation than a *trans*, and therefore, an upfield shift of about 4 ppm is expected if the alkyl segment involves conformational disorder. Above the glass transition temperature, a C–C-bond can be either in *trans* conformation (*t*) or disordered (*d*) undergoing rapid interconversions between *trans* and *gauche*. With regard to the conformation of the two neighbouring bonds, the carbon under observation is part of a *tt*-, *td*- or *dd*-arrangement, which gives rise to NMR signals at about 34, 32 and 30 ppm, respectively. Cheng et al. have found mainly *tt*-arrangements in the crystals, *td* in the LC-phase and *dd* in the isotropic phase of polyethers [38].

The influence of the spacer length, the type of mesogen, and the temperature on the spacer conformation of PEI has been published recently [13]. Fig. 12 represents the ^{13}C NMR signals of the methylene groups of PEI **2** $n = 16$ in the frozen smectic LC-phase (a) and in the smectic-crystalline phase (b). The resonances overlap severely, so that they have to be separated by deconvolution (details in Ref. [13]). In addition to the signal of the γ-carbon at 27 ppm, two or three components of the inner methylene carbons can be detected in the range of 30–34 ppm, which represent the different arrangements. One can see that the spacer segments in the LC-structure adopt mainly *td*-conformations, corresponding to an alternate-*trans* model [39]. The *dd*-component indicates disorder in the smectic-LC structure. In contrast, the spacer conformation of the smectic-crystalline phases exhibits a larger variety. It should be noted that both, the amount of ordered *tt*-sequences and completely disordered *dd*-arrangements increase. This observation corresponds with the detection of the SAXS, assuming that the *tt*-sequences represent mainly the crystal lamellae, while the disordered interlamellar regions contain *dd*-sequences.

4. Conclusion

As a result of the regular sequence of rigid, polar mesogens and flexible, non-polar spacers, the poly(ester imide)s (PEI) studied form various smectic layer structures in the liquid and solid state.

If the LC-phase is lost completely due to a sufficient prolongation of the spacer, or if a sample is crystallised isothermally at a temperature above the monotropic LC-phase, the smectic-crystalline phase develops directly out of the isotropic melt with a three-dimensional spherulitic morphology. The observation of spherulites growing slowly within the isotropic matrix excludes an intermediate LC-formation. The spherulites are constructed of lamellar stacks with a *d*-spacing of 100–400 Å, each of the lamellae consisting of a number of smectic-crystalline layers.

During the transition from the smectic LC-phase to the smectic-crystalline phase, the same lamellar structure with a *d*-spacing of 100–400 Å is formed, giving rise to a long period reflection in the SAXS. However, this process is induced by one-dimensional nuclei in the disclination centres of the LC-texture, resulting in a two-dimensional crystal growth. As a result of long-range chain reptations and diffusions, which are necessary in generating backfoldings at the lamella surface, the smectic layer order may be lost to some extent in the interlamellar regions.

The X-ray fibre patterns demonstrate that the PEI based on aminobenzoic acid form exclusively orthogonal smectic phases (S_A, S_B, and S_E), whereas the PEI derived from aminocinnamic acid produce tilted phases (S_C, S_H). The layerline shape of the MAXS reflections indicate a poor lateral correlation of the smectic LC-layers due to undulations.

The spacer segments in the frozen LC-phase exhibit a rather uniform conformation, in which stable *trans*-bonds alternate with mobile bonds that undergo rapid *trans–gauche* jumps. The smectic-crystalline phase contains *trans–trans*-conformations that can be attributed to the higher-ordered smectic-crystalline lamellae and completely disordered sequences in the amorphous, interlamellar regions.

Acknowledgements

The author wishes to thank Prof. H.R. Kricheldorf for providing the polymer samples synthesised by Dr N. Probst. Thanks also to L. Good for proof-reading the manuscript.

References

[1] Flory PJ. Proc R Soc 1956;234A:73.
[2] Majnusz J, Catala JM, Lenz RW. Eur Polym J 1983;19:1043.
[3] Krigbaum WR, Hakemi H, Kotek R. Macromolecules 1985;18:965.
[4] Ebert M, Herrmann-Schönherr O, Wendorff J, Ringsdorf H, Tschirner P. Makromol Chem Rapid Commun 1988;9:445.
[5] Jackson Jr WJ. Br Polym J 1980;12:154.
[6] Griffin BP, Cox MK. Br Polym J 1980;12:147.
[7] Blumstein A, Gauthier M, Thomas O, Blumstein RB. Faraday Discuss Chem Soc 1985;79:33.
[8] Watanabe J, Hayashi M, Nakata Y, Niori T, Tokita M. Prog Polym Sci 1997;22:1053.
[9] Ober ChK, Jin J-I, Lenz RW. Prog Polym Sci, 59. Berlin: Springer, 1984. p. 103.
[10] Kricheldorf HR, Schwarz G, de Abajo J, de la Campa J. Polymer 1991;32:942.
[11] Kricheldorf HR, Probst N, Wutz C. Macromolecules 1995;28:7990.
[12] Gray GW, Goodby JWG. Smectic liquid crystals, New York: Leonard Hill, 1984.
[13] Wutz C, Schleyer D. Polym Sci: Part B: Polym Phys 1998;36:2033.
[14] Pardey R, Zhang A, Gabori PA, Harris FW, Cheng SZD, Adduci J, Facinelli JV, Lenz RW. Macromolecules 1992;25:5060.
[15] Pardey R, Shen D, Gabori PA, Harris FW, Cheng SZD, Adduci J, Facinelli JV, Lenz RW. Macromolecules 1993;26:3687.
[16] Pardey R, Wu S, Chen J, Harris W, Cheng S, Keller A, Aducci J, Facinelli V, Lenz RW. Macromolecules 1994;27:5794.
[17] Kricheldorf HR, Probst N, Schwarz G, Wutz C. Macromolecules 1996;29(12):4234.
[18] Wutz C. Polymer 1998;39(1):1.
[19] Avrami M. J Chem Phys 1939;7:1109.
[20] Avrami M. J Chem Phys 1940;8:212.
[21] Avrami M. J Chem Phys 1941;9:117.
[22] Wutz C, Schäfer R. Mol Cryst Liq Cryst 1999;326:75.
[23] Stein RS, Rhodes MB. J Appl Phys 1960;31:1873.
[24] Hashimoto T, Nakai A, Shiwaku T, Hasegawa H, Rojstaczer S, Stein RS. Macromolecules 1989;22:422.
[25] Donald AM, Windle AH. Liquid crystalline polymers, Cambridge: Cambridge University Press, 1992.
[26] Yoon Y, Ho R-M, Moon B, Kim D, McCreight KW, Li F, Harris FW, Cheng SZD, Percec V, Chu P. Macromolecules 1996;26:3421.
[27] Blumstein A, Vilasagar S, Ponrathnam S, Clough SB, Blumstein RB. J Polym Sci Polym Phys Ed 1982;20:877.
[28] Wutz C, Gieseler D, Maevis T, Stribeck N. Molecular order of the mesogens in smectic poly(ester imide) fibers. In preparation.
[29] Wutz C. Mol Cryst Liq Cryst 1997;307:175.
[30] Watanabe J, Hayashi M. Macromolecules 1988;21:278.
[31] Thomas EL, Wood B. Faraday Discuss Chem Soc 1985;79:229.
[32] Tokita M, Takahashi T, Hayashi M, Inomata K, Watanabe J. Macromolecules 1996;29:1345.
[33] Wutz C, Stribeck N, Gieseler D. Investigation of molecular order and phase trasitions of smectic poly(ester imide)s by means of small angle X-ray scattering macromolecules. Submitted for publication.
[34] Stribeck N, Wutz C. Layer morphology of a poly(ester imide) LCP in different solid states. Submitted for publication.
[35] Wunderlich B, Grebowicz J. Thermotropic mesophases and mesophase transitions of linear, flexible macromolecules, Adv Polym Sci. Berlin: Springer, 1984.
[36] Zhao SR, Schaper A, Ruland W. Acta Polym 1993;44:173.
[37] Tonelli E. NMR spectroscopy and polymer microstructure, New York: VCH Publishers, 1989.
[38] Cheng J, Yoon Y, Ho R-M, Leland M, Guo M, Cheng SZD, Chu P, Percec V. Macromolecules 1997;30:4688.
[39] Leisen J, Boeffel C, Spiess HW, Yoon DY, Sherwood MH, Kawasumi M, Percec V. Macromolecules 1995;28:6937.